Towards an Efficient Digital Twin Framework for Fiber Composite Structures Using Optimal Sensor Placement Techniques

VARAKINI SANMUGADAS and RAKESH K. KAPANIA

ABSTRACT

Structural health monitoring (SHM) is a critical component in the safe and efficient operation of aerospace structures. Preliminary studies were carried out to investigate the suitability of sparse sensor measurements to estimate the response of fiber composite structures and predict their performance. The displacement response was approximated using a linear combination of a set of basis vectors, where the basis vectors were extracted from a snapshot matrix of the structure's response under various loads. The coefficients of the basis vectors were assessed in real time using the sensor measurements at sparse locations chosen based on the pivot locations of the QR algorithm. This displacement map is then leveraged to compute critical SHM parameters such as the buckling load. The proposed method was applied to a fiber composite plate subjected to in-plane buckling loads. It was shown that the displacement vectors were mapped with $L2$-norm errors of mean 0.003% using measurements at just six locations, leading to stress distribution and buckling load estimations with very small errors.

INTRODUCTION

Fiber composites are gaining popularity in aerospace structures due to their advantages in lightweight design, stiffness tailoring, thermal resistance, and corrosion protection. For these materials to be safely and effectively integrated into commercial applications, robust structural health monitoring (SHM) systems are essential. They collect real-time data during the operation of a structural system and use these data to make inferences about its present state and predict future states. The estimation procedure typically involves components such as physics-based digital models, inverse-modeling approaches, and data-driven models. In this work, the focus is on obtaining strain data from optimally placed sensors, which will then be used to estimate the complete displacement profile of the structure. The availability of the displacement profile would

Varakini Sanmugadas, Postdoctoral Research Associate, Department of Aerospace and Ocean Engineering, Virginia Polytechnic Institute and State University, Blacksburg, VA, USA. Email: svarakini@vt.edu. Rakesh K. Kapania, Mitchell Professor, Department of Aerospace and Ocean Engineering, Virginia Polytechnic Institute and State University, Blacksburg, VA, USA. Email: rkapania@vt.edu.

enable the computation of quantities of interest such as stress distribution and buckling load factor. An SHM framework involving *optimal sensor placement* (OSP) and efficient computation of some quantities of interest (QoI) are discussed.

The concept of OSP has been explored extensively in the literature for applications such as structural health monitoring [1], network management [2], and environmental monitoring [1]. In structural health monitoring, an ideal sensor placement prioritizes optimizing data for inverse modeling, often using a least-squares data fitting approach to match test data to numerical predictions [3, 4].

The current work explores a related, but slightly different approach for predicting full-field measurements from sparse data. We used finite element-based expressions for quantities of interest (QoI) such as the buckling load parameter and stress resultants, but replaced the displacement vector with an approximation. This displacement approximation consisted of a set of basis vectors and load-dependent coefficients. The coefficients can be assessed real-time during the operation of the system based on sparse sensor measurements. This leads to the interesting problem of determining the optimal sensor locations. Manohar et al. [5] demonstrated an innovative method for identifying optimal sensor locations based on QR decomposition, allowing the complete reconstruction of images from selected data points. They showed that the pivot locations of the QR decomposition of the matrix of basis vectors correspond to the optimal sensor placement locations. In this work, we leverage this idea to obtain a map of the mid-plane displacements of a structure and use it to compute the QoI. The projection vectors for mapping the displacement are formed from a snapshot matrix containing the structure's response under different loading conditions, and an affine form of the stress-strain tensors and the stiffness matrices isolates load-dependent scalars from the load-independent matrices that can be pre-computed and stored.

OPTIMAL SENSOR PLACEMENT (OSP) THEORY

The sparse sensor placement approach described by Manohar et al. [5] operates by collecting sample data related to a specific application or model, extracts a tailored basis vector $\mathbf{\Psi_r} \in \mathbb{R}^{n \times r}$, and identifies the significant features that have to be captured to express the signal $\mathbf{x}$ as a linear combination of $\mathbf{\Psi_r}$ with coefficient vector $\mathbf{a} \in \mathbb{R}^r$. This relationship is given by

$$\mathbf{x} = \mathbf{\Psi_r a}. \tag{1}$$

The main aspect of this approach is the determination of a measurement matrix $\mathbf{C} \in \mathbb{R}^{p \times n}$ that is optimized to capture data related to the defining features needed to compute $\mathbf{a}$ such that $\mathbf{x}$ can be recovered from $\mathbf{\Psi_r}$. Mathematically, this matrix comprises of canonical basis vectors $\mathbf{e}_j \in \mathbb{R}^n$ with zeros everywhere except for a unit entry at index j, corresponding to a point measurement. This definition is given by Eq. (2) and it is related to the measurements $\mathbf{y}$ as stated in Eq. (3).

$$\mathbf{C} = [\mathbf{e}_{\gamma 1} \; \mathbf{e}_{\gamma 1} \; ... \; \mathbf{e}_{\gamma p}] \tag{2}$$

$$\mathbf{y} = (\mathbf{C \Psi})\mathbf{a} = \mathbf{\Theta a}. \tag{3}$$

The objective of the OSP approach is to find the set of rows of Ψ_r that optimizes the condition number associated with the inversion of $\mathbf{\Theta}$. This ensures that the sensitivity of the inverse of $\mathbf{\Theta}$ to errors in the input is as small as possible. With these optimal measurements, Eq. (3) can be used to compute $\mathbf{a}$, which could then be used to reconstruct the full-order response $\mathbf{x}$ using Eq. (1). See Ref. [6–8] for more details on extracting $\mathbf{\Psi}$ and Ref. [5] for details on the method to identify the optimal sensor locations using the QR algorithm.

FIBER COMPOSITE PLATE SUBJECTED TO IN-PLANE BUCKLING LOADS

Displacement Approximation

In accordance with Eq. (1), the displacement vector $\mathbf{q} \in \mathbb{R}^n$ for n degrees of freedom, is approximated in terms of a set of projection basis vectors $\bar{\mathbf{q}} \in \mathbb{R}^{n \times r_s}$ and coefficient vector $\mathbf{c} \in \mathbb{R}^{r_s}$, resulting in the over-determined system of equations,

$$\mathbf{q} = \bar{\mathbf{q}}\mathbf{c}. \tag{4}$$

Here, $\mathbf{c}$ has to be chosen such that the difference between the true displacement $\mathbf{q}$ and its approximation is minimized. However, in the current problem, the full-order response is not known. The estimation has to be made based on measurements available at only n_p degrees of freedom, leading to the new system of equations,

$$\begin{bmatrix} q_1^{\mathrm{M}} \\ q_2^{\mathrm{M}} \\ \vdots \\ q_p^{\mathrm{M}} \end{bmatrix}_{n_p \times 1} \approx \begin{bmatrix} | & | & & | \\ \bar{q}_1^{\mathrm{P}} & \bar{q}_2^{\mathrm{P}} & \cdots & \bar{q}_{r_s}^{\mathrm{P}} \\ | & | & & | \end{bmatrix}_{n_p \times r_s} \begin{bmatrix} c_1 \\ c_2 \\ \vdots \\ c_p \end{bmatrix}_{r_s \times 1} = \bar{\mathbf{q}}^{\mathrm{P}}[\mathbf{c}] \tag{5}$$

where $\bar{\mathbf{q}}^{\mathrm{P}}$ is the matrix formed by n_p number of rows of $\bar{\mathbf{q}}$ where the row index is chosen according to Ref. [5]. The q^{M} vector elements in Eq. (5) are the measurements taken at optimal locations. Here, we chose $p = r_s$.

Quantities of Interest

STRESS RESULTANTS

The stress resultant vector $\mathbf{N}_i^p$ can be expressed as,

$$\mathbf{N}_i^p = \mathrm{diag}\left[t\tau, \tfrac{t^3}{12}\tau, \tfrac{t^3}{12}\tau\right], \quad \text{where, } \tau = \begin{bmatrix} \sigma_{xx} & \sigma_{xy} \\ \sigma_{xy} & \sigma_{yy} \end{bmatrix} \tag{6}$$

An equivalent compact affine form for τ was derived by the authors in Ref. [8].

BUCKLING PARAMETER

Buckling can generally be formulated as an eigenvalue problem of the form,

$$[\mathbf{K} - \lambda\mathbf{G}]\{\mathbf{q}\} = \{\mathbf{0}\}, \tag{7}$$

where $\mathbf{K} \in \mathbb{R}^{n \times n}$ is the elastic stiffness matrix of the structure, and $\mathbf{G} \in \mathbb{R}^{n \times n}$ is the geometric stiffness matrix induced by the applied compressive loads. The buckling load is given by λ, and the mode shape is provided by the corresponding eigenvector, $\mathbf{q}$. The formulation in Eq. (7) assumes tensile loads to be positive.

The linear stiffness matrix does not depend on the external loads acting on the system. Future work will consider changes to it due to changes in the material stiffness distribution due to factors such as damage. The geometric stiffness matrix depends on the applied loads and can be written in the affine form presented by the authors in Ref. [8].

Structural Health Monitoring Framework

The proposed SHM framework has two steps: (1) offline phase, where the set of basis vectors are generated and the load-independent components of the QoI expressions are computed and stored, and optimal locations for the sensors are identified and equipped to take physical measurements, and (2) online phase, where load-dependent components of the QoI expressions are assessed in real-time using the sensor data. In this preliminary study, it was assumed that displacement data was readily available at the optimal locations.

CASE STUDY: ANALYSIS OF A TOW-STEERED FIBER COMPOSITE PLATE

Model Details

A simply supported 0.3 m $\times$ 0.3 m flat plate (Fig. 1) was considered for this study. It was made of a symmetric, variable angle tow (VAT) fiber composite material with 8 plies and each ply had a thickness of 0.127 mm. The material properties considered for the lamina are, $E_1 = 181$ GPa, $E_2 = 10.273$ GPa, $G_{12} = 7.1705$ GPa, and Poisson's ratio, $\nu_{12} = 0.28$. The laminate configuration shown in Fig. 1(b) corresponds to $[\pm\langle 45|45\rangle, \langle 0|0\rangle, \langle 90|90\rangle]_{2n}$ for this study. The structure is subjected to uniaxial displacements. The static analysis was carried out with the boundary conditions shown in Fig. 1(c).

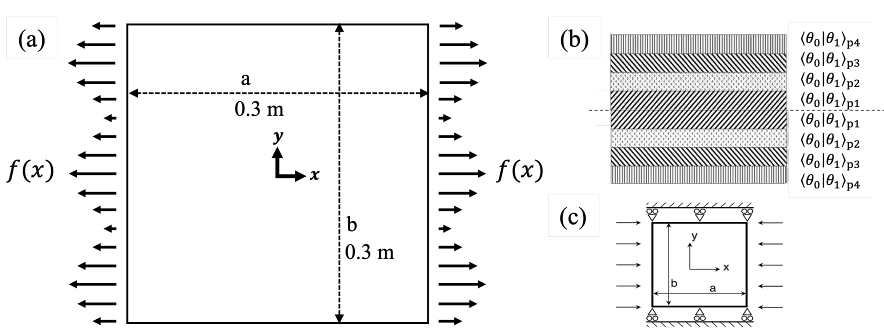

Figure 1. Case study model: (a) plate dimensions, (b) cross-section of composite laminate, showing laminate configuration θ_0 and θ_1, associated with the ply p_i, and (c) boundary conditions for static analysis.

In this preliminary study, only uniaxial loads acting on the two opposing edges of the fiber composite plate in Fig. 1 were considered. The loads were parameterized as shown in Fig. 1(a), where $f(y)$ is given in Eq. (8), a function chosen from Ref. [9]. The variation of the load $f(y)$ along the y-axis is determined based on the parameters μ and ω.

$$f(y) = \mu + 0.05\sin(\omega|y|) \tag{8}$$

The normalized critical buckling load parameter $\bar{\lambda}$ for this structure is computed as,

$$\bar{\lambda} = \frac{P_1 a^2}{E_1 b t^3} \tag{9}$$

where,

$$P_1 = \lambda_1 \int_{b/2}^{b/2} N_{xx}(a, y)\mathrm{d}y \tag{10}$$

Here, P_1 is the critical buckling load defined by the in-plane stress resultant N_{xx} and lowest eigenvalue λ_1 of the generalized eigenvalue problem in Eq. (7). Young's modulus is given by E_1. The structure will buckle for $\bar{\lambda} < 1$.

Dataset for Loading Conditions

The dataset should be generated to cover different loading conditions the structure could experience. Sampling points corresponding to 3200 load patterns were generated for $\mu \in [0.1, 1.5]$ and $\omega \in [0.1, 20]$, out of which 2400 (*training set*) were used for creating the reduced basis vectors and the remaining 800 (*testing set*) were used to test the developed model. The Latin Hypercube Sampling (LHS) technique was used to choose μ and ω values for the load patterns in this dataset. This method ensures that the parameters are chosen optimally to capture the potential loading scenarios described by Eq. (8). The space-filling nature of LHS is demonstrated in Fig. 2.

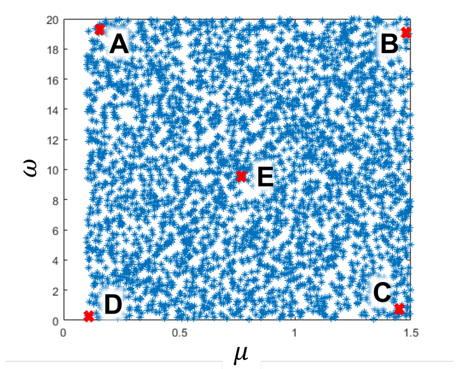

Figure 2. Sample points μ versus ω chosen using Latin Hypercube Sampling. Sampling points A-E with coordinates $\langle \mu, \omega \rangle$: A $\langle 0.14, 19.37 \rangle$, B $\langle 1.48, 19.09 \rangle$, C $\langle 1.46, 0.57 \rangle$, D $\langle 0.11, 0.29 \rangle$, E $\langle 0.75, 9.83 \rangle$

.

DISCUSSION

The order of the basis vectors $\mathbf{\Psi}$ are chosen based on singular value decomposition (SVD) of the snapshot matrix and the most dominant r_s left singular vectors according to the singular value tolerance [7]. Three different SVD tolerances δ of 99%, 99.9%, and 99.999% were considered in this study, resulting in basis vectors of $r_s = 4, 5, 6$ respectively. The errors in predicting the static displacement profile of the testing set are given in Fig. 3. The error is defined in Eq. (11) and uses the Euclidean norm, or the $L2$-norm, of the displacement vector and its approximation errors.

$$\text{Error} = \frac{||\mathbf{q}_{\text{FOM}} - \mathbf{q}_{\text{ROM}}||}{||\mathbf{q}_{\text{FOM}}||} \times 100 \tag{11}$$

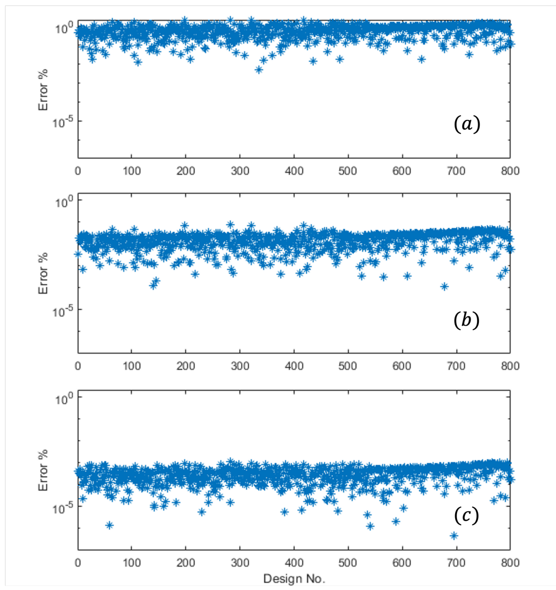

Figure 3. Errors associated with different SVD tolerance δ and reduced basis orders r: (a) $\delta = 99\%,\ r = 4$, (b) $\delta = 99.9\%,\ r = 5$, and (c) $\delta = 99.999\%,\ r = 6$.

The set of basis vectors with $r = 6$ was chosen for the study to be conservative. The probability density function plots of displacement approximation errors in Fig. 4(a) further demonstrate that the chosen approximation is able to reproduce the true displacement profile effectively with errors centered around a mean of 0.0002 % and 0.0003 % for the training and testing sets, respectively. The buckling model was assembled using the approximate displacement profile and the percentage errors associated with the buckling load parameters were computed in a manner similar to the displacement errors. The plot of the error distribution for the testing set is provided in Fig. 4(b). As evident from the distributions shown here, the errors are quite low with a mean of -0.003%.

The stress resultants N_{xx}, N_{yy} and N_{xy} were also computed using the approximate displacement vector. The approximate stress distributions for points A-E (Fig. 2) were compared with the stress distribution from the full-order model and the errors are presented in Fig. 5. Figure 5 demonstrates that the present model is able to capture all the components of the stress resultants with errors of comparatively insignificant order.

Future work will extend this study to more load cases, including varying magnitudes and shear loads. Another important aspect of developing a comprehensive SHM digital

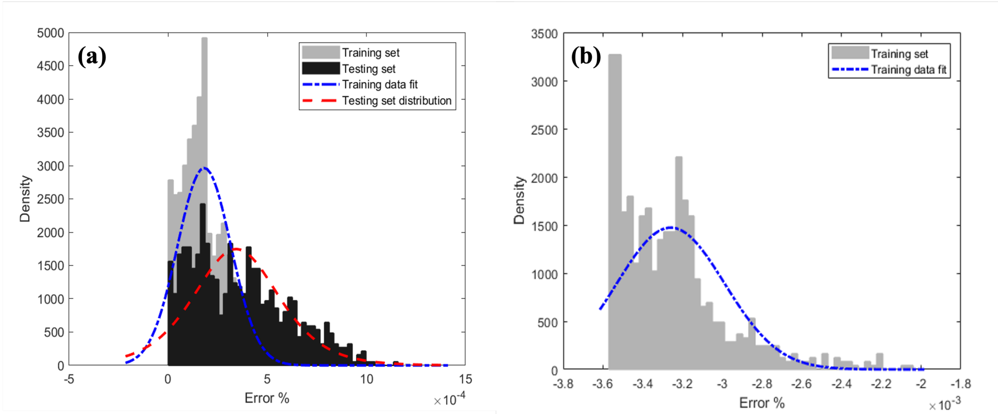

Figure 4. Probability density function (PDF) for errors due sparse sensor measurements in: (a) displacements, and (b) buckling load parameters.

twin is updating the model to reflect changes in its intrinsic properties due to factors such as damage and aging of the structure. In addition, the framework must account for uncertainties, especially in measurements, and incorporate models that are robust under the influence of different sources of errors. Also, in the current work, it was assumed that the displacement data can be easily obtained at the optimal sensor locations. However, for structures such as aircraft, responses are generally obtained as strain measurements through embedded strain gauges and some locations may be inaccessible for measurements. Future work will tailor the proposed approach to these practical requirements.

CONCLUDING REMARKS

Preliminary studies were conducted to investigate the applicability of an optimal sensor placement technique involving QR decomposition to deduce the full-field displacement response of fiber composite structures from sparse measurements. It was shown that within the scope of this study, the approach performed very well in capturing the displacement fields, as well as the stress resultants and buckling load parameters under various patterns of uniaxial loads applied on the structure. This shows that the framework proposed in this study is promising for structural health monitoring applications. Future work will focus on investigating more practical models with complex load cases and developing this framework into a robust digital twin useful for SHM.

REFERENCES

1. Wogrin, S., A. Singh, D. Allaire, O. Ghattas, and K. Willcox. *From Data to Decisions: A Real-Time Measurement–Inversion–Prediction–Steering Framework for Hazardous Events and Health Monitoring*, Springer International Publishing, Cham, pp. 195–227.
2. Jiang, J.-A., J.-C. Wang, H.-S. Wu, C.-H. Lee, C.-Y. Chou, L.-C. Wu, and Y.-C. Yang. 2020. "A Novel Sensor Placement Strategy for an IoT-Based Power Grid Monitoring System," *IEEE Internet of Things Journal*, 7(8):7773–7782.

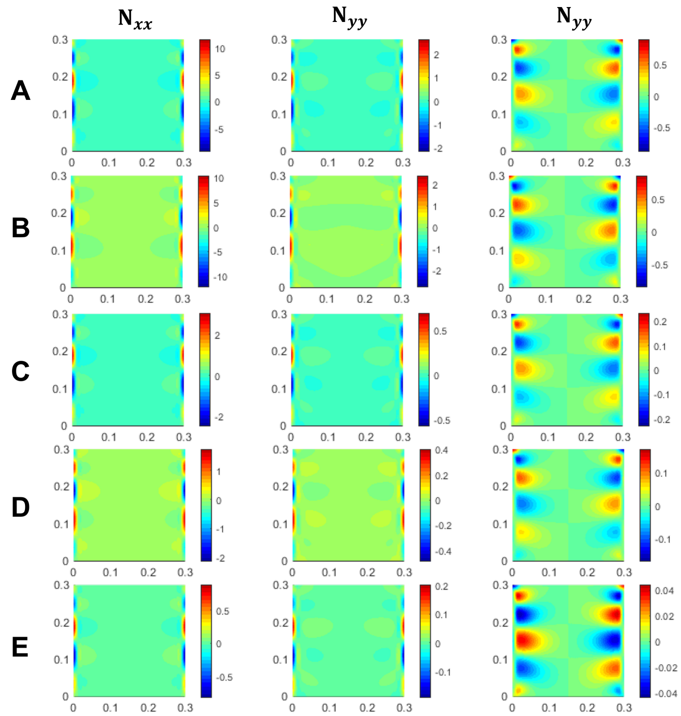

Figure 5. Stress resultant error distributions associated with approximation of N_{xx}, N_{yy} and N_{xy} for the structure subjected to loads associated with sample points A-E.

3. Shkarayev, S., R. Krashantisa, and A. Tessler. September, 2001. “An Inverse Interpolation Method Utilizing In-Flight Strain Measurements for Determining Loads and Structural Response of Aerospace Vehicles,” 3rd IWSHM Conference, Stanford, CA.
4. Pham, J. V., O. Ghattas, N. T. Clemens, and K. E. Willcox. 2025. “Real-Time Aerodynamic Load Estimation for Hypersonics via Strain-Based Inverse Maps,” *AIAA Journal*, 63(1):91–101.
5. Manohar, K., B. W. Brunton, J. N. Kutz, and S. L. Brunton. 2018. “Data-Driven Sparse Sensor Placement for Reconstruction: Demonstrating the Benefits of Exploiting Known Patterns,” *IEEE Control Systems Magazine*, 38(3):63–86.
6. Benner, P., S. Gugercin, and K. Willcox. 2015. “A Survey of Projection-Based Model Reduction Methods for Parametric Dynamical Systems,” *SIAM Review*, 57(4):483–531.
7. Sanmugadas, V., M. Agarwal, P. Borwankar, and R. K. Kapania. 2025. “Parametric Model Order Reduction for Structural Optimization of Fiber Composite Structures,” *AIAA Journal*, 63(5):2064–2079.
8. Sanmugadas, V. 2024. *Reduced Order Modeling for Efficient Stability Analysis in Structural Optimization*, Ph.D. thesis, Virginia Polytechnic Institute and State University, Blacksburg, VA, available at `https://hdl.handle.net/10919/121347`.
9. Go, M.-S., H.-K. Noh, and J. Hyuk Lim. 2025. “Real-Time Full-Field Inference of Displacement and Stress from Sparse Local Measurements using Physics-Informed Neural Networks,” *Mechanical Systems and Signal Processing*, 224:112009.